Lithos 236–237 (2015) 203–211

Contents lists available at ScienceDirect

Lithos

journal homepage: www.elsevier.com/locate/lithos

Geochronology and geochemistry of rhyolites from Hormuz Island, southern Iran: A new record of Cadomian arc magmatism in the Hormuz Formation

Narges Sadat Faramarzi [a,b,*], Sadraddin Amini [a,c], Axel Karl Schmitt [c], Jamshid Hassanzadeh [d], Gregor Borg [e], Kevin McKeegan [c], Seyed Mohammad Hosein Razavi [a], Seyed Mohsen Mortazavi [f]

[a] Department of Geology, Kharazmi University, 49 Mofatteh Avenue, Tehran 15614, Islamic Republic of Iran
[b] Department of Research and Development (R & D), Pars Kani Co., Tehran 1593663415, Islamic Republic of Iran
[c] Department of Earth, Planetary, and Space Sciences, University of California, Los Angeles, CA 90095-1567, USA
[d] Division of Geological and Planetary Sciences, California Institute of Technology, Pasadena, CA 91125, USA
[e] Institute of Geosciences and Geography, Martin-Luther-University Halle, Wittenberg, Germany
[f] Department of Geology, Hormozgan University, Bandar Abbas, Islamic Republic of Iran

ARTICLE INFO

Article history:
Received 21 December 2014
Accepted 26 August 2015
Available online 12 September 2015

Editor: Lin Chung Sun-

Keywords:
Hormuz
Rhyolite
Geochronology
Geochemistry
Cadomian arc magmatism

ABSTRACT

Hormuz Island, a salt-gypsum dome in the Persian Gulf in southern Iran, is a complex halotectonic melange comprising evaporites, carbonates, volcanic and volcaniclastic rocks, as well as low-grade metamorphic and sedimentary rocks. Based on trace element (including rare earth elements REE) compositions of whole rocks and zircon, Hormuz rhyolites are inferred to have formed from subduction-related magmas generated in an active continental margin setting. Ion microprobe analyses of zircon crystals yielded concordant U–Pb ages with weighted mean $^{206}Pb/^{238}U$ age of 558 ± 7 Ma (juvenile zircons in contrast to those from previous magmatic episodes or xenocrysts) along with younger and older discordant ages which likely represent Pb loss and the presence of xenocrystic domains, respectively. Trace element ratios and in particular REE patterns of juvenile zircon from Hormuz rhyolites indicate crystallization from continental crustal source rocks typical for subduction environments. The concordant $^{206}Pb/^{238}U$ zircon age agrees with ages obtained from most other structural zones of Iran which indicate regional consolidation of igneous basement during the Neoproterozoic to Early Cambrian. Furthermore, Hormuz rhyolite ages and compositions correlate with counterparts that co-evolved along the northern margin of Gondwana, and are now preserved along the southern coast of the Persian Gulf. Hormuz rhyolites erupted synchronously with the deposition of carbonates and evaporites, suggesting that volcanism occupied an extensional backarc or retroarc setting. Such depositional environments predominated in the northern Gondwana continental margin where convergent (Proto-Tethyan) and extensional (Najd) tectonic regimes coexisted.

1. Introduction

During the Neoproterozoic to Early Cambrian, Iran was located at the northeastern margin of the Gondwana supercontinent (Balaghi Einalou et al., 2014; Berberian and King, 1981; Ghavidel-Syooki, 1995; Hassanzadeh et al., 2008; Stocklin, 1968). Contemporaneous deposition of evaporites and carbonates along Gondwana supercontinental margins is recorded in Iran in several locations (Hormuz Formation, Ravar Formation, Rizu-Dezu series, and stratigraphically informal Cambrian volcanic sediments). These may be correlative to other evaporites and carbonates with known occurrences in northwestern India (Bilara and Hanseran groups), Pakistan (Salt Range in Panjab), Oman (Ara group and Fara formation), the United Arab Emirates (e.g., Das, Dalma, Qarnian, Zirkouh, Arzanah Islands), Saudi Arabia (Wadi Fatima series), Jordan (Arabba complex), Qatar, Yemen, eastern Siberia, and Iberia (Alsharhan and Nairn, 1997; Amthor et al., 2003; Bowring et al., 2007; Das Gupta, 1996; Husseini, 1990; Kumar, 1999; Ramezani and Tucker, 2003; Sánchez-García et al., 2010). Evaporites and carbonates of the Hormuz Formation exposed along the Persian Gulf and southern Iran have been identified in over 200 salt-gypsum domes in the eastern Zagros Mountains (e.g., Bosak et al., 1998; Liaghat, 2002) with Hormuz Island being one of the salt-gypsum domes of the eponymous formation. During the island's emergence from the Persian Gulf, the Hormuz dome transported blocks of exotic sedimentary, igneous, and metamorphic rocks to the surface. Various types of metamorphic rocks of anchi-

* Corresponding author at: Department of Geology, Kharazmi University, 49 Mofatteh Avenue, Tehran 15614, Islamic Republic of Iran. Tel.: +98 9122548994; fax: +98 2188663352.
E-mail address: nargesfaramarzi@yahoo.com (N.S. Faramarzi).

http://dx.doi.org/10.1016/j.lithos.2015.08.017
0024-4937/

metamorphic to amphibolite-facies grade (which may be derived from unexposed basement rocks) have been reported from different parts of the Hormuz Formation (e.g., Bosak et al., 1998; Kent, 1970). The presence of hydrothermal minerals in some parts of the formation has also been attributed to hydrothermal fluids produced by rift-related magmatic activity (Ala, 1974; Nasir et al., 2003; Schröder et al., 2003).

Here, we focus on rhyolites of the Hormuz Island that are exposed as isolated sub-circular enclaves (~40 to 480 m in diameter) surrounded by evaporite deposits. The rhyolites have undergone dramatic changes during their upward passage along with the salt dome and are consequently highly altered due to protracted contact with salt. The extent of the resulting alteration makes the identification of the nature, origin, and age of the Hormuz rhyolites difficult. Rock units within the Hormuz Formation have been estimated to be of various ages, ranging from Precambrian to Jurassic (e.g., Ahmadzadeh-Heravi et al., 1990; Ala, 1974; Alavi, 2004; De Bockh et al., 1929; Elyasi et al., 1977; Ghazban and Motiei, 2007; Harrison, 1930; Hurford et al., 1984; Nasir et al., 2008; Pilgrim, 1908, 1924; Player, 1969; Stocklin, 1968), and because of the intense alteration, zircon geochronology and geochemistry is here identified as the most promising method to unravel the age and formation conditions of these rhyolites. We thus present the first high spatial resolution data on the U–Th–Pb isotopic and chemical compositions of zircon crystals extracted from Hormuz Formation rhyolites which allow a correlation of Hormuz rhyolites with other volcanic deposits preserved along the southern coast of the Persian Gulf.

2. Geological background

The Hormuz Island is an oval-shaped island covering 45 km^2 of the Strait of Hormuz. In its central part (~2 km in diameter) it shows a concentric structure with salt, gypsum, and anhydrite evaporite deposits (Fig. 1). These evaporites show primary layering caused by the presence of ferruginous agglomerates and Fe–Mn bearing clays. The central parts of the island are surrounded by salt containing abundant rock fragments of various sedimentary and volcanic lithologies. These fragments include purple and black shales (from few centimeters to 1 m in diameter), black and white dolomites (0.1 to 2 m in diameter), limestone to sandy limestone, Fe oxide layers, volcanoclastic and volcanic rocks (tuff, rhyolite, and trachyte ranging from ~0.0013 to 0.25 km^2 in area). The larger enclaves in the salt occur isolated and they seem to have been transported to the surface along with the salt dome. A brecciated ferruginous ring (thickness between 18 and 117 m) surrounded by young sediments (varying in thickness from a few meters to 2 km) wraps around the island. Commonly sedimentary and igneous fragments of Hormuz Island are affected by low grade (prehnite facies) regional metamorphism which predates their surficial emplacement (Fig. 1).

The rhyolite fragments on Hormuz Island contain quartz, sanidine, sodic plagioclase, biotite, and hornblende (mostly altered to chlorite) as major minerals which often are porphyritic in texture. Zircon, tourmaline, apatite, monazite, Fe–Ti oxides, and rarely epidote are accessory minerals (Fig. 2A). Secondary halite, anhydrite, and sylvite are observed in the groundmass of the rhyolites and sometime even as precipitates in fluid inclusions hosted by quartz and biotite phenocrysts (Fig. 2B).

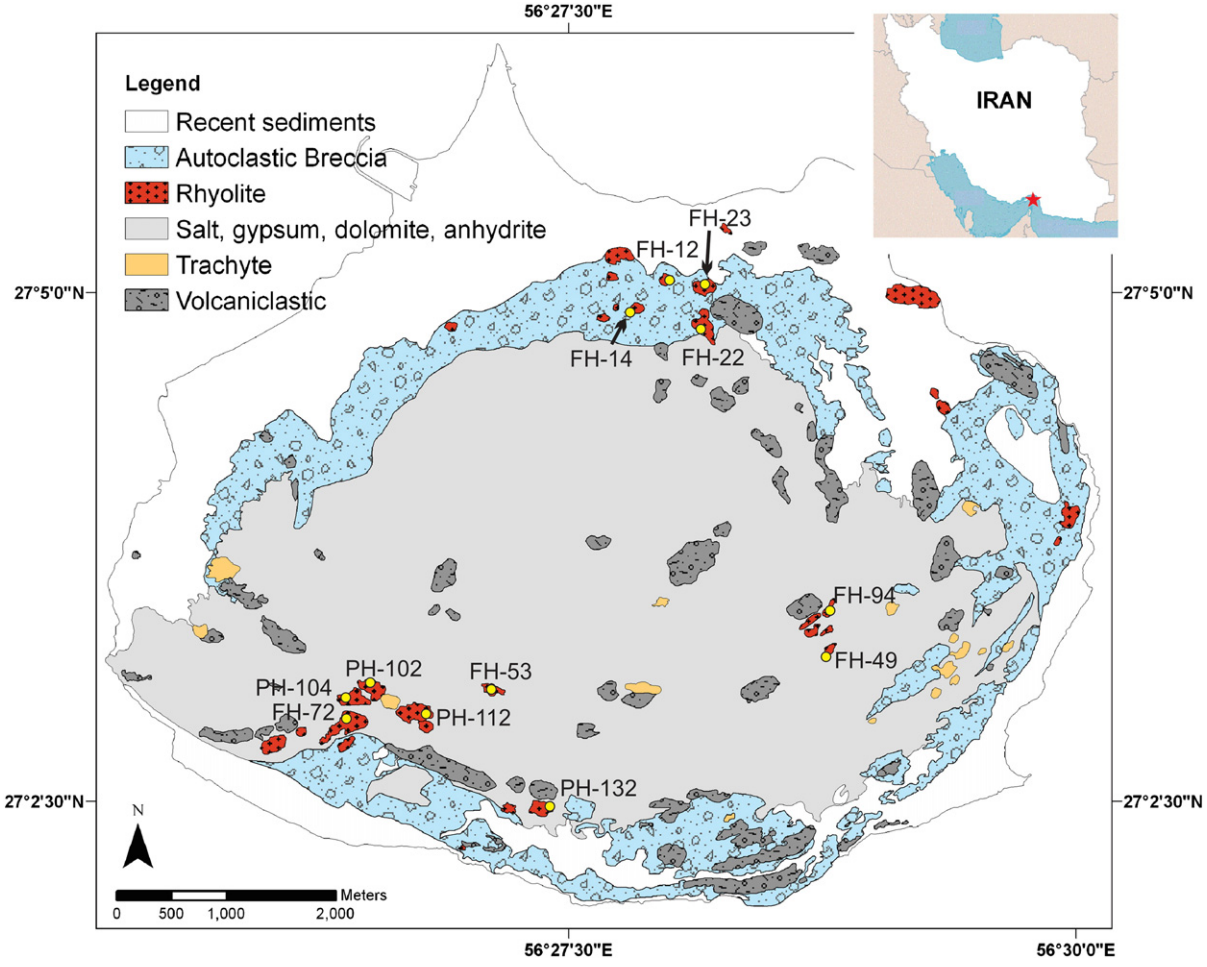

Fig. 1. Simplified geological map of Hormuz Island showing the Hormuz rhyolites and their positions in relation to other rocks.

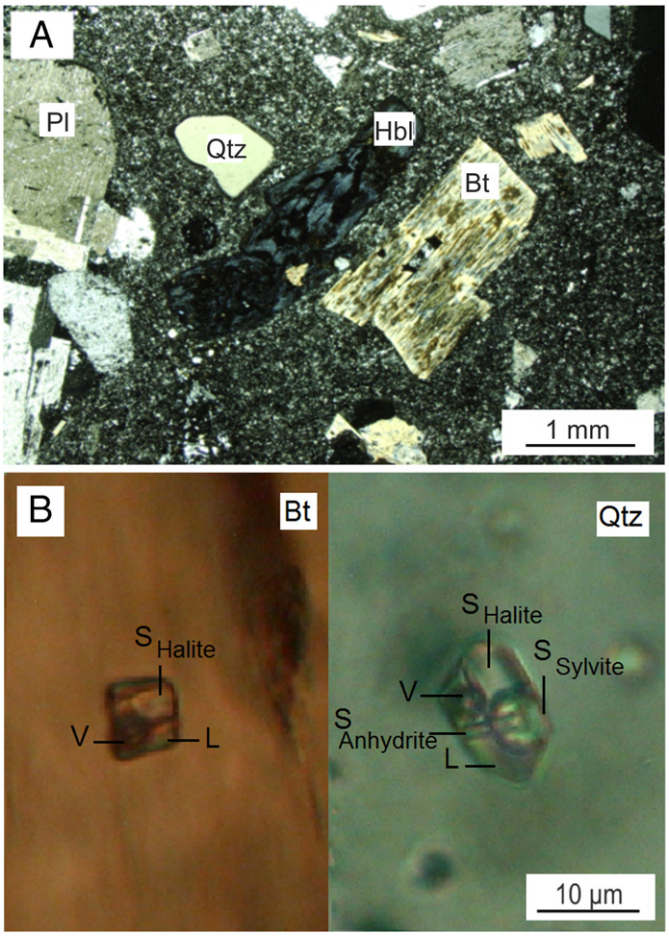

Fig. 2. A) Photomicrograph of the rhyolitic sample of FH-22 showing a porphyritic texture. B) Fluid inclusions in the same sample showing vapor (V), liquid (L) and three solid (S) phases of halite, anhydrite and sylvite in quartz and vapor (V), liquid (L) and one solid (S) phases of halite in biotite.

3. Materials and methods

This study is based on the results from field work, microscopy, whole rock geochemistry, fluid inclusion analysis of quartz, geochemistry, and geochronology of zircon from Hormuz rhyolites. After microscopic studies, 12 least altered rhyolite samples were selected for whole rock analysis, of which three samples were selected for zircon separation. In order to perform whole rock analyses, the samples were powdered to <74 μm using an agate mill, and the powders were analyzed by X-ray fluorescence (XRF; for major oxides) and inductively coupled plasma-mass spectrometry (ICP-MS; for minor and trace elements) methods. The XRF analyses were carried out using a Panalytical Axios instrument with Super Q analytical software at University of the Free State (South Africa). The accuracy was <1% for SiO_2 and Al_2O_3 and 5% (relative) for the other oxides. The ICP-MS analyses were conducted at ACME laboratories (Canada) following a lithium metaborate/tetraborate fusion and nitric acid digestion of 0.2 g sample powder. In addition another 0.5 g split was digested in aqua regia to determine precious and base metals. The detection limit for trace elements (including the rare earth elements REE) by ICP-MS is ~0.01 ppm.

Following zircon separation using conventional liquid and magnetic techniques, clear euhedral zircon grains were hand-selected, mounted in epoxy, sectioned and polished using abrasives, and coated with carbon. The carbon coated disk was used for cathodoluminescence (CL) imaging at the University of California, Los Angeles (UCLA) using a Leo 1430 VP SEM. Major and minor elemental compositions of 40 selected points on the same zircon crystals were analyzed by electron microprobe analysis (EMPA) using a JEOL 8200 SuperProbe at UCLA.

For secondary ion mass spectrometry (SIMS) studies a separate mount was prepared in the same manner as above, except for applying a conductive ~100 Å gold layer for SIMS analyses. U, Pb, and Th isotopic measurements were performed in spot analysis of rims of 19 zircon crystals using the CAMECA ims1270 ion microprobe at UCLA. Analytical methods followed the procedures described by Quidelleur et al. (1997) and Schmitt et al. (2003). An ~15 nA primary ion beam of mass-filtered ^{16}O ions was focused to an ~15–20 μm diameter spot and secondary ions were analyzed with the mass spectrometer tuned to a mass resolving power of 5000 and the energy bandpass set to 50 eV. Following a pre-sputtering period of ~180 s, each analysis collected data for 10 magnet cycles from mass 203.5 (background) to 254 (UO^+). The sample chamber was flooded with oxygen at $\sim 3 \times 10^{-5}$ Torr to enhance secondary Pb ionization. The reported weighted mean ages are based on $^{206}Pb/^{238}U$ ages corrected for instrumental relative sensitivity bias using zircon reference AS3 (1099.1 Ma; Paces and Miller, 1993). Common lead corrections were made using the measured intensities of ^{204}Pb and a model composition based on Stacey and Kramers (1975). All age uncertainties in the text are reported at the 2σ level; the tables list 1σ errors for ease of calculation. The same mount was subsequently used for trace element analysis of 16 previously age dated zircons using the CAMECA ims1270 at UCLA. SIMS trace element analysis spots and age spots occupy different domains within the zircon crystals analyzed, but uninterrupted oscillatory zonation suggests continuous crystallization. Zircon trace element data were corrected for instrumental relative sensitivity bias using 91500 reference zircon (Wiedenbeck et al., 1995).

4. Whole rock geochemistry

The Hormuz rhyolites contain 67.6–74.6 wt.% SiO_2, high levels of K_2O (4.36–10.8 wt.%), and comparatively low amounts of Na_2O (0.44–4.35 wt.%) (Table A1; Supplementary Appendix). Since the major element, and especially alkali elements, classification is dubious due to the intense alteration of the Hormuz rhyolites, immobile trace elements have been used to constrain their tectonic environment of formation. Based on Co vs Th (Hastie et al., 2007; Fig. 3A), and Ta/Yb vs Th/Yb (Pearce, 1982; Fig. 3B) diagrams, they classify as high-K calc-alkaline and shoshonitic rhyolites. On the Pearce et al. (1984) discrimination diagrams (e.g., Ta vs Yb; Fig. 3C), rhyolites plot in the "volcanic arc" domain and show characteristics of the volcanic rocks generated in active continental margin (ACM) based on Schandl and Gorton (2002) diagrams (e.g., Th/Yb vs Ta/Yb; Fig. 3D).

5. Geochronology

The width and length of the analyzed Hormuz rhyolite zircon crystals are 38–200 and 115–368 μm, respectively. Zircon width to length ratios range from approximately 1:2 to 1:10. Most crystals show some evidence for internal zonation with zircon interiors being colorless, transparent, and normal birefringence. Interiors are largely homogeneous and lack inclusions (e.g., apatite or monazite). The outer zircon domains mantling these clear interiors are darker, less transparent, and with lower birefringence. CL textures show narrowly spaced and uninterrupted oscillatory zoning (Fig. A1; Supplementary Appendix).

Based on the CL images (Fig. A1), the ages of 19 points of euhedral zircons of the rhyolitic samples FH14, FH22, and FH94 were determined using ion microprobe analysis (Fig. 4A and B; Table A2). Because of the comparatively imprecise ^{207}Pb-based ages after correction for common Pb, we concentrated on the $^{206}Pb/^{238}U$ ages (Fig. 4B) to extract coherent age populations using the "Unmix Ages" algorithm in Isoplot 4.1 (Ludwig, 2012). The number of components was incrementally increased until the goodness of fit showed no further improvement. The resulting five components correspond to the peaks and shoulders visible in the $^{206}Pb/^{238}U$ age probability density plot (Fig. 5). Six analyses

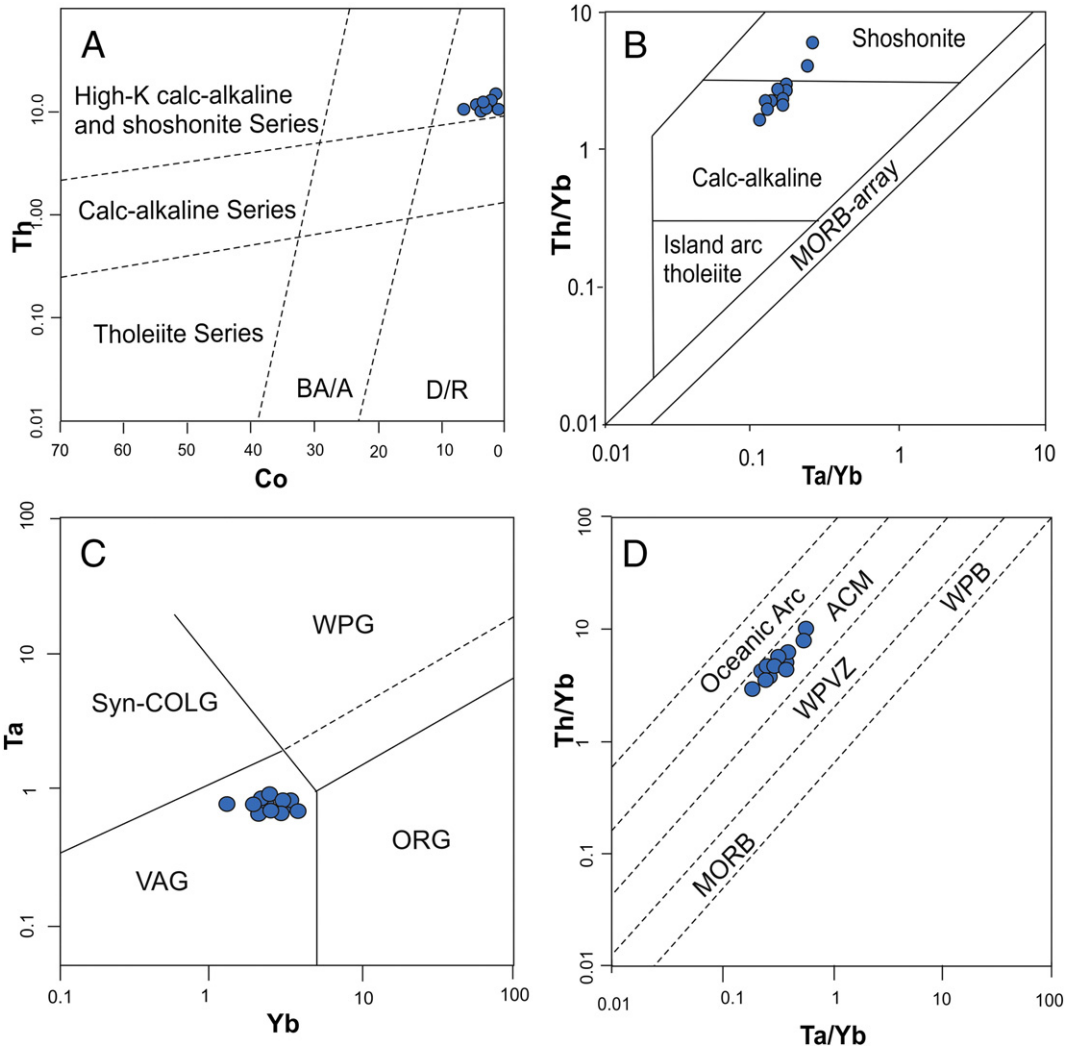

Fig. 3. Hormuz rhyolites on (A) Co vs Th (Hastie et al., 2007) diagram, and (B) Ta/Yb vs Th/Yb (Pearce, 1982) diagram classify as calc-alkaline and slightly shoshonite rhyolites. On the (C) Ta vs Yb discrimination diagram (Pearce et al., 1984) they plot in the "volcanic arc" domain (VAG) and on the (D) Th/Yb vs Ta/Yb diagram (Schandl and Gorton, 2002) is plotted in the active continental margin (ACM).

(corresponding to two components) show discordant younger ages ranging from ca. 270 to 500 Ma (Fig. 5). These crystal domains are interpreted as impacted by metamictization and Pb-loss (see below). The next older population comprises six spot analyses (omitting one analysis with high Th/U) which yielded concordant U–Pb ages with a weighted mean $^{206}Pb/^{238}U$ age of 558 ± 7 Ma (95% confidence; including decay constant uncertainties) and a mean square of weighted deviates (MSWD) of 0.86 (Fig. 4A). These are termed juvenile zircons, and likely represent the original crystallization age. The remaining seven analyses (again, resolvable as two components) define a heterogeneous older category with $^{206}Pb/^{238}U$ ages between ca. 600 and 800 Ma. They are also marginally resolvable from the juvenile component by slightly older but comparatively imprecise $^{207}Pb/^{206}Pb$ dates, and are tentatively interpreted as basement-derived xenocrysts. An indistinguishable but less precise upper intercept age of 567 ± 17 Ma (MSWD = 1.08; n = 19; Fig. 4B) is obtained by regressing the entire data set which is supportive of the interpretation that the younger ages represent Pb loss.

6. Zircon chemistry

Zircon major and trace element analyses were performed targeting the same coherent growth domains dated by SIMS analysis. Major and some minor and trace components analyzed by EMPA (Table A3) also include additional crystals that were not dated, but which represent the same textural diversity as the dated crystals. Trace elements determined by SIMS (Table A4) are directly linked to the categorization based on geochronology. Differences in Th and U abundances between SIMS trace element analysis spots and age spots on the same grain (Tables A2 and A4) presumably result from internal chemical zonation.

Average HfO_2 in the studied zircons (0.96–1.73 wt.%, Table A3) is consistent with values reported by Hoskin et al. (2000) and Wang et al. (2010). The spatial distribution of HfO_2 was explored on a subset of textually representative zircons by EPMA. In some cases, HfO_2 increases from the cores towards the margins of the zircons (Fig. A2). Such an increase is expected in magmatic zircon (Benisek and Finger, 1993; Caironi et al., 2000) crystallizing along a retrograde temperature path. Because these crystals were not dated, we are unsure about the timing of crystallization, but interpret the HfO_2 data as supportive of the textural evidence (the prevalence of oscillatory zoning) that all Hormuz zircons are magmatic in origin.

Th/U in xenocrystic, juvenile, and Pb loss affected zircons closely overlap and range from 0.3 to 0.7, 0.3 to 0.8, and 0.2 to 0.5, respectively (Table A4). For all crystals, these ratios are significantly higher than the <0.01 limit characteristic for metamorphic zircons (e.g., Rubatto, 2002), and they completely overlap with the 0.1–1 range typical for magmatic zircons (e.g., Belousova et al., 2002). The averages of total REE (∑REE) and Y in xenocrysts (1638 and 2525 ppm, respectively), juvenile (1631 and 2507 ppm, respectively), and Pb loss affected zircons (1507 and

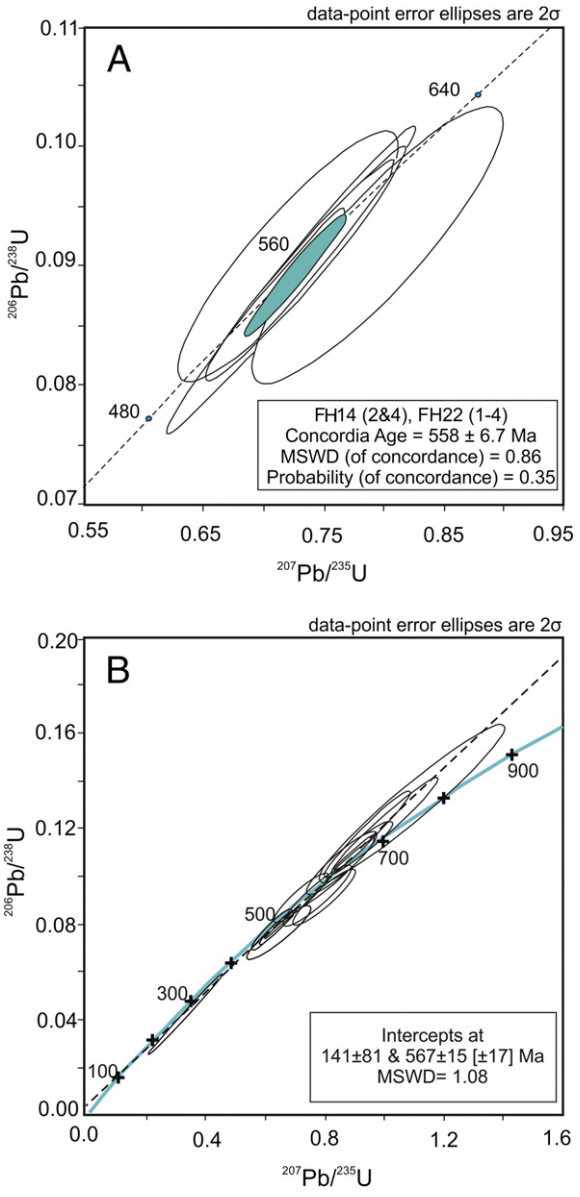

Fig. 4. (A) Concordia diagram and (B) discordia diagram showing ion microprobe zircon U–Pb data from the Hormuz rhyolites.

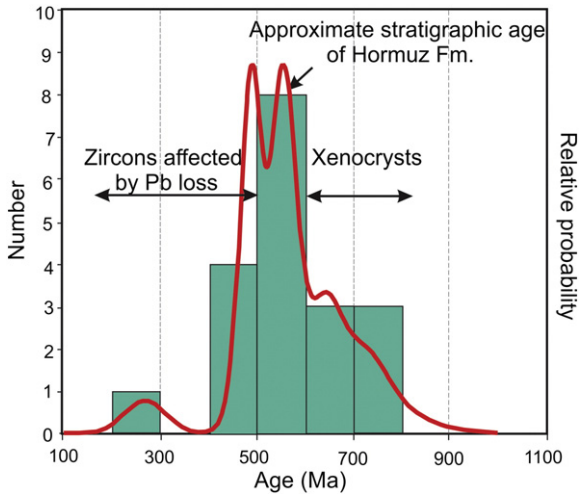

Fig. 5. Relative probability of the Hormuz rhyolite U–Pb ages diagram. The ages of older than 558 ± 7 Ma are related to basement and younger ones are probably resulted due to Pb loss.

2292 ppm respectively; Table A4) fall in the range of unaltered magmatic zircons of granitic rocks (e.g., Hoskin and Ireland, 2000; Hoskin and Schaltegger, 2004). Chondrite-normalized (McDonough and Sun, 1995) zircon REE abundances for the three age groups of studied zircons show patterns that steeply-rise from low LREE towards high HREE with a positive Ce-anomaly and a negative Eu-anomaly (Fig. 6). Average $(Sm/La)_N$ in xenocrysts (146), juvenile (147) and Pb loss affected zircons (125) from the Hormuz rhyolites as well as their average $(Lu/Gd)_N$ (xenocrysts = 29, juvenile = 28 and Pb loss affected zircons = 38) are similar to continental crustal zircons whose $(Sm/La)_N$ and $(Lu/Gd)_N$ averages range from 57 to 547 and 16 to 74, respectively (Hoskin and Schaltegger, 2004).

The Ce abundances of xenocrysts (2.9–29.4 ppm), juvenile (2.8–9.5 ppm) and Pb loss affected zircons (3.1–10.7 ppm; Table A4) largely overlap and are within the <50 ppm range typical for magmatic zircon (e.g., Hoskin et al., 2000; Sano et al., 2002). Higher Ce abundances have been associated with the presence of inherited cores (Griffin et al., 2002) or metamorphic xenocrysts (Hidaka et al., 2002) for which we have no evidence. The average positive Ce anomaly (expressed as Ce/Ce*) is lowest for the xenocrysts (7.9), and increases in the juvenile (12.0), and Pb loss affected zircons (14.8), whereas their average Eu/Eu* ratios show the opposite trend (xenocrysts = 0.08, juvenile = 0.06 and Pb loss affected zircons = 0.05; Table A4). The average concentrations of P in xenocrysts, juvenile, and Pb loss affected zircons are indistinguishable at 339, 399, and 377 ppm, respectively. The amounts of Li, Be, B, F, Na, Mg, Al, Ca, Sc, V, Cr, Mn, Fe, Sr, Ba, and Ta are usually below detection (Table A4), which is typical for unaltered magmatic zircon (Ballard et al., 2002; Hoskin et al., 2000).

Zircon trace element compositions have been used to broadly classify their magmatic–tectonic regimes. Comparing the three groups of Hormuz zircons to fields for mid oceanic rifts, continental hot spots, and oceanic hot spots (Iceland) in Gd/Yb vs Sm and Yb, Yb vs U, Y vs U/Yb, and Hf vs U/Yb diagrams (Grimes et al., 2007; Carley et al., 2014; Fig. 7) shows distinct differences, and strong affinities to compilations of zircons from typical continental source rocks.

7. Zircon thermometry

Whole-rock Zr abundances in Hormuz rhyolites vary between 80 and 152 ppm. This translates into zircon saturation temperatures (Boehnke et al., 2013) between 672 °C and 789 °C. Because of their porphyritic texture, whole-rock Zr abundances yield zircon saturation temperatures that somewhat underestimate the actual onset of zircon

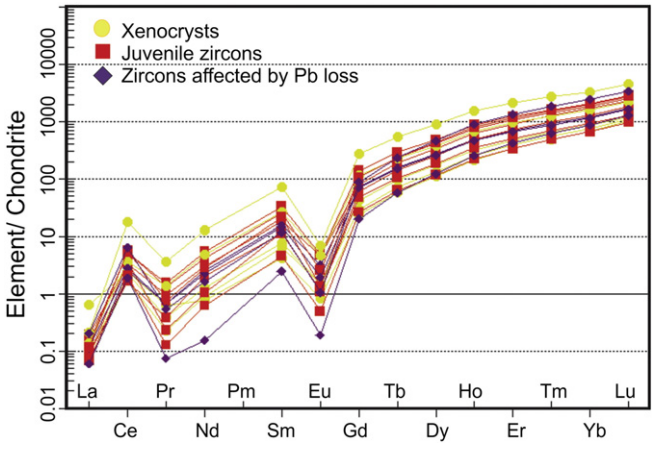

Fig. 6. Chondrite-normalized REE abundances of xenocrysts, juvenile and Pb loss affected zircons from Hormuz rhyolites against the data given by McDonough and Sun (1995).

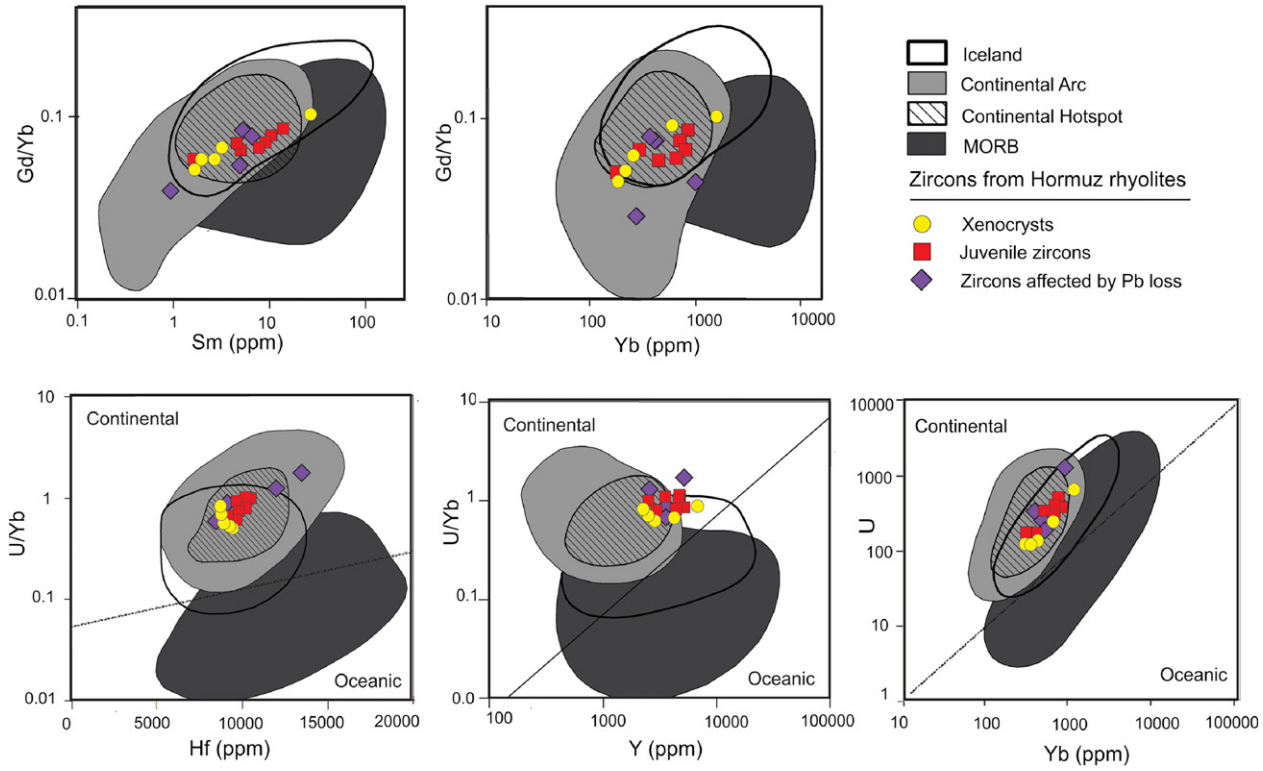

Fig. 7. A global comparison of zircons from the Hormuz rhyolites based on trace element composition on Sm (ppm) and Yb (ppm) vs Gd/Yb, Yb (ppm) vs U (ppm), Y (ppm) vs U/Yb and Hf (ppm) vs U/Yb discrimination diagrams (Carley et al., 2014; Grimes et al., 2007). Dashed lines delineate continental and oceanic (MORB) compositional fields.

crystallization in these magmas. Moreover, these temperatures need to be considered with caution because they depend on the abundance of alkali elements and Ca which are likely altered. For comparison, temperatures of zircon crystallization estimated from Ti-in-zircon abundances are 682–709 °C (xenocrysts), 629–726 °C (juvenile zircons) and 551–702 °C (zircons affected by Pb loss). These temperatures are based on the calibration of Ferry and Watson (2007) and assume Ti and Si activities of 1.0. They represent minimum temperatures if Ti activities were significantly <1 (likely because of the absence of rutile), but for comparison purposes with data for continental arc zircons we assume an activity of 1 as was done for global compilations of Ti-in-zircon data. Based on this comparison, Hormuz zircons interpreted to be affected by Pb loss have the lowest average temperatures, and xenocrysts the highest, albeit with significant overlap with the juvenile Ti-in-zircon temperature range (Fig. 8). Average Ti for Hormuz rhyolite zircon falls below the average for continental arcs although the ranges overlap. We interpret this to reflect the evolved composition of the Hormuz rhyolites compared to the dominantly intermediate compositions (e.g., Mt. St. Helens) used in the compilation by Carley et al. (2014).

8. Discussion

Commonly, Pb loss from zircon affects metamict crystals or crystal domains whereas Pb diffusion in crystalline zircon is exceedingly slow under normal conditions of crustal storage (Cherniak and Watson, 2001). There, are, however, indications that salt can considerably enhance Pb mobility even for crystalline zircon: Pb loss measured for polished grains of Sri Lanka gem zircon immersed in molten NaCl (Lee et al., 1997) exceeded Pb volume diffusion measured for zircon surrounded by a mixture of $PbSO_4$ and finely ground zircon (Cherniak and Watson, 2001). This might indicate that salt plays a role in accelerating the extraction of Pb from crystalline zircon. Pb loss from metamict zircon would result in an inverse correlation between U abundance and age; this, however, is not supported by the trace element and age data for Hormuz zircon (Tables A2 and A4). Furthermore, there is no indication from the trace element data for significant chemical differences between juvenile and Pb-loss affected crystals. We therefore suspect that local exposure to saline fluids, as evident from saline fluid inclusions in major mineral phases, might control the mobility of Pb without significantly altering the chemical composition of zircon.

The age obtained for a coherent group of Hormuz zircons (558 ± 7 Ma) is in agreement with the U–Pb zircon age of 547 ± 6 Ma reported

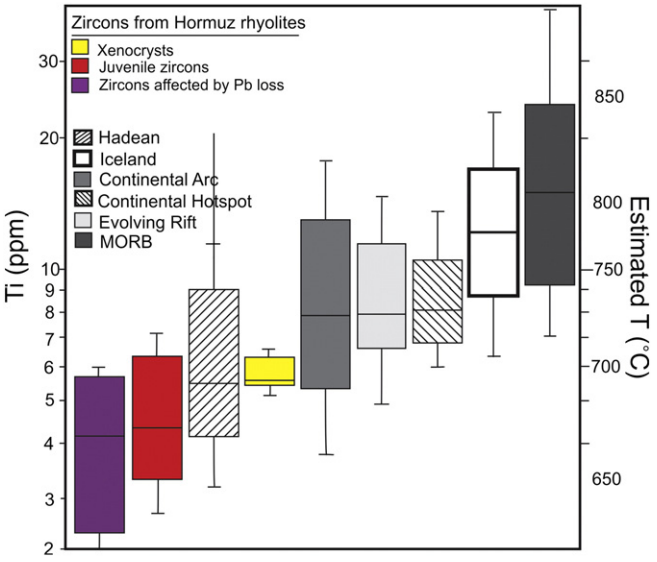

Fig. 8. Comparison of Ti in xenocrysts, juvenile and Pb loss affected zircons in the Hormuz rhyolites with global zircon populations on discrimination diagram in the style of Carley et al. (2014). Temperatures are calculated using the method of Ferry and Watson (2007) in Ti and Si activities of 1.0. The lower and the upper parts of each whisker are limited to 10th and 90th percentile respectively. The lower boundaries of boxes are 25th percentile and the upper boundaries present the 75th percentile. The line inside boxes presents the median Ti content.

for leucogranitic enclaves in the Jahani salt diapir of the southeastern Zagros Mountains, another locality belonging to the Hormuz Formation (Alavi, 2004). Indistinguishable U–Pb zircon ages also exist for ashes of the Ara Group and Fara Formation in Oman (541–547 Ma and 542–547 Ma respectively; Brasier et al., 2000; Bowring et al., 2007), rhyolites of the Araba Complex in Jordan (542–550 Ma; McCourt and Ibrahim, 1990), and the Mutki granites in Turkey (545.5 ± 6.1 Ma; Ustaömer et al., 2009). The stratigraphic correlation of the Hormuz Formation in Iran with the Ara Group in Oman, which we propose here for the first time, implicates conformity of both units in time and depositional environment (Fig. 9). Allen (2007) associated the volcanic activity of the Ara formation with arc magmatism. This magmatism was caused by the subduction of the Proto-Tethyan Ocean that resulted in the formation of a retro-arc in present-day Oman. According to Allen (2007), the evaporitic Hormuz–Ara belt was compressed due to its position between subducting Proto-Tethyan oceanic crust along the east margin of Gondwana and the megasuture margin of the Arabian–Nubian shield. The presence of ca. 525–547 Ma metamorphic rocks and magmatic activity in central Iran confirm the aforementioned subduction process (Hassanzadeh et al., 2008; Ramezani and Tucker, 2003; Shafaii Moghadam et al., 2013). Whole-rock and zircon geochemistry of Hormuz rhyolites are entirely consistent with origin in a volcanic arc in an active continental margin setting. An active continental setting is also supported by the presence of xenocrysts which have very similar trace element compositions as the juvenile zircons, suggesting crustal assimilation during Hormuz rhyolite volcanism. High temperature metamorphism associated with subduction and magmatism has been reported for local outcrops of the Hormuz Formation (e.g., Bosak et al., 1998; Kent, 1970), but there is no evidence of such metamorphism on the island itself where existing metamorphic indicator minerals are limited to prehnite. Crustal anatexis and/or assimilation therefore must have occurred at a much deeper crustal level which is not exposed on Hormuz.

Due to the complexity caused by halokinetic movements in the salt-gypsum dome of Hormuz Island, it is impossible to clarify the stratigraphic position of the studied rhyolites merely based on the contact relationships of the rocks in the field. There are, however, some indications that volcanism and deposition of thick evaporite strata were coeval: secondary halite, anhydrite, and sylvite are pervasive in the groundmass of the rhyolites, and exist as fluid inclusions hosted by quartz and biotite phenocrysts, whereas hydrothermal sanidine and hematite (presently undated) fill joints and cracks in some Hormuz dolomites. Therefore, it is conceivable that volcanism was at least in part concurrent with the deposition of evaporites and carbonate sediments.

Based on our geochronological and geochemical data for Hormuz rhyolites and zircon crystals extracted from them, we postulate the following regional correlations which also take into account geochemical similarities between the depositional environment of the Hormuz Formation and deposits elsewhere along the northern margin of Gondwana:

1) The zircon ages for Hormuz Island (558 ± 7 Ma) together with U–Pb zircon ages of igneous rocks from the Hormuz formation in the Jahani salt diapir (547 ± 6 Ma; Alavi, 2004) and data obtained from all structural zones in Iran (with the exception of Kopet Dagh; Ramezani and Tucker, 2003; Horton et al., 2008; Hassanzadeh et al., 2008; Shafaii Moghadam et al., 2013; Balaghi Einalou et al., 2014) reveal consolidation of igneous basement at about 600 to 520 Ma. In fact, magmatic and tectonic environments recorded by rhyolites of the Hormuz formation might be linked to other localities along the former northern margin of Gondwana;
2) The Hormuz Formation is not only lithologically similar to synchronous rocks in Oman (Fig. 9), the United Arab Emirates, Saudi Arabia, Qatar, Bahrain, Yemen, Pakistan, Turkey, and eastern and southern Siberia (which were situated on the margins of Gondwana at that time), but also shows similar U–Pb zircon ages obtained for

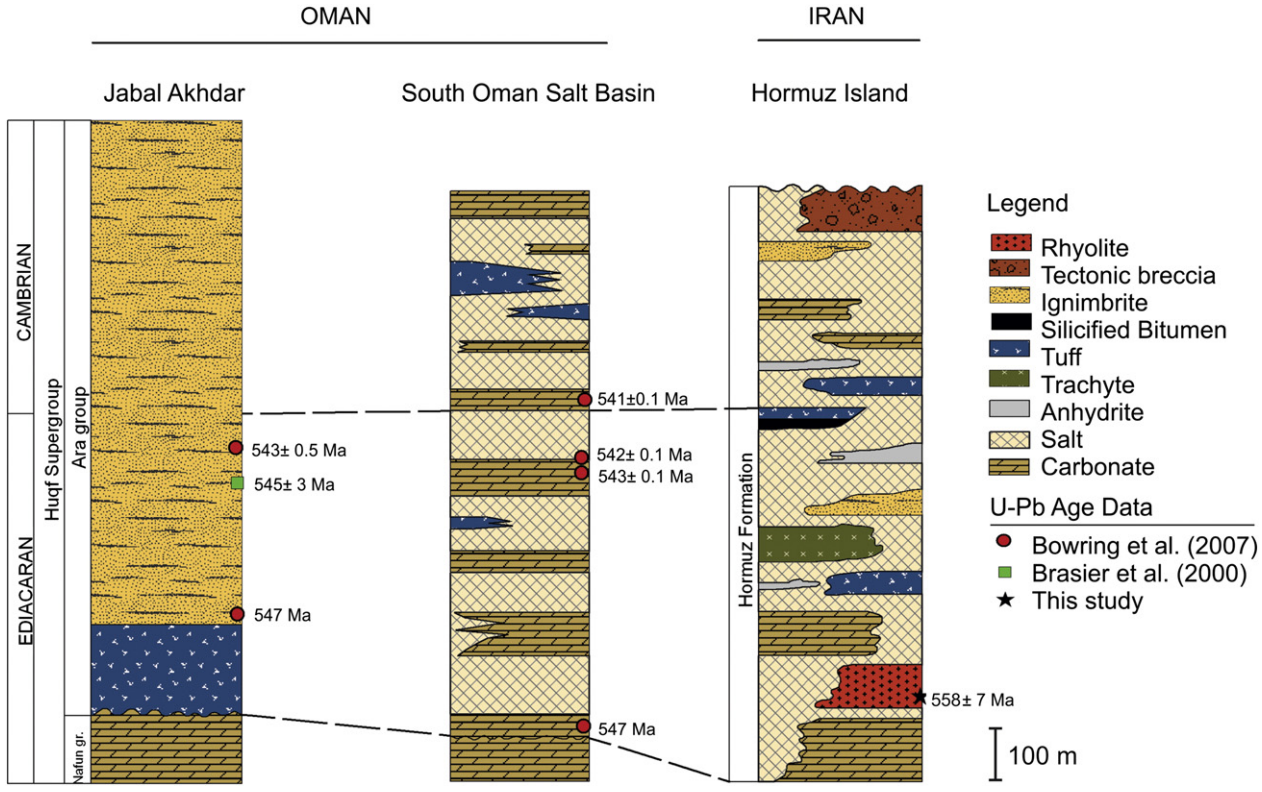

Fig. 9. Lithostratigraphy of Neoproterozoic to Early Cambrian rocks in Oman (Amthor et al., 2003; Bowring et al., 2007) and Hormuz Island in Iran along with U–Pb ages of Ara ash beds within carbonate strata (Bowring et al., 2007; Brasier et al., 2000) and Hormuz rhyolites.

volcanic rocks with those of the Ara Group and Fara Formation in Oman (541–547 Ma and 542–547 Ma, respectively; Brasier et al., 2000; Bowring et al., 2007; Fig. 9), rhyolites of the Araba Complex in Jordan (542–550 Ma; McCourt and Ibrahim, 1990), and the Mutki granites in Bitlis, Turkey (545.5 ± 6 Ma; Ustaömer et al., 2009).

3) Collectively, these Cadomian (Ediacaran–Cambrian) volcanic and plutonic rocks share geochemical characteristics that are indicative of arc-related magmatism along the northern margin of Gondwana.

9. Conclusions

The Hormuz Formation is known as one of the most complicated rock units of Iran. In this paper, we propose that this complexity is not only due to halokinetic movements but also due to the protracted contact of rocks with salt. In Hormuz Island, the salt effect not only severely overprinted the chemical composition of rocks and minerals but also partially mobilized Pb from zircon. Based on the age distribution of zircon crystals in Hormuz rhyolites, we have distinguished a juvenile population from populations that are xenocrystic (older) and affected by Pb loss (younger). The lack of correlation between U abundance and Pb-loss suggests that saline fluids may be a controlling factor in Pb mobilization and producing unreasonably young ages for the rhyolites of the Hormuz Formation. However, saline fluids appear to have no significant effects on the distribution of trace and REE elements in zircon. This suggests that these elements in zircon are reliable indicators for the tectonic environment of zircon formation, even in highly altered host rocks. The global comparison of zircons from rhyolites in Hormuz based on trace and REE elements, as well as the whole rock results, reveals a magmatic origin in an active continental margin setting. Moreover, stratigraphic evidence suggests that volcanism occupied an extensional backarc or retroarc environment which predominated also in other parts of the northern Gondwana continental margin. The similarity of ages obtained in this study with those of most structural zones of Iran and other localities along the former northern margin of Gondwana verifies magmatic basement consolidation in the region via subduction-related magmatism during Neoproterozoic to Early Cambrian.

Supplementary data to this article can be found online at http://dx.doi.org/10.1016/j.lithos.2015.08.017.

Acknowledgment

The first author would like to greatly appreciate Dr. Abdolrahim Houshmandzadeh, Dr. Thomas Johannes Degen and Sabine Walther for all their helpful suggestions. Editorial suggestions by Prof. Sun-Lin Chung are appreciated. We are very grateful to Dr. Hadi Shafaii Moghadam and an anonymous reviewer for their constructive reviews of the manuscript, and Prof. Christoph Gauert who provided us the XRF analysis. Support from the Department of Earth, Planetary, and Space Sciences of UCLA, the Martin-Luther-University Halle-Wittenberg Germany, the University of the Free State of South Africa, the Ministry of Sciences Research and Technology of Iran, and the University of Kharazmi is acknowledged. The ion microprobe facility at UCLA is partly supported by a grant from the Instrumentation and Facilities Program, Division of Earth Sciences, National Science Foundation.

References

Ahmadzadeh-Heravi, M., Hoshmandzadeh, A., Nabavi, M.H., 1990. New concepts of Hormuz formation's stratigraphy and the problem of salt diapirism in south Iran. Proceeding of Symposium on Diapirism with Special Reference to Iran. 1, pp. 1–21.

Ala, M.A., 1974. Salt diapirism in southern Iran. American Association of Petroleum Geologists Bulletin 58, 1758–1770.

Alavi, M., 2004. Regional stratigraphy of the Zagros fold-thrust belt of Iran and its proforeland evolution. American Journal of Science 304, 1–20.

Allen, P.A., 2007. The Huqf Supergroup of Oman: basin development and context for Neoproterozoic glaciation. Earth-Science Reviews 84, 139–185.

Alsharhan, A.S., Nairn, A.E.M., 1997. Sedimentary Basins and Petroleum Geology of the Middle East. Elsevier, Amsterdam (843 pp.).

Amthor, J.E., Gratzinger, J.P., Schröder, S., Bowring, S.A., Ramezani, J., Martin, M.W., Matter, A., 2003. Extinction of Cloudina and Namacalathus at the Precambrian–Cambrian boundary in Oman. Geology 31, 431–434.

Balaghi Einalou, M., Sadeghian, M., Zhai, M., Ghasemi, H., Mohajjel, M., 2014. Zircon U–Pb ages, Hf isotopes and geochemistry of the schists, gneisses and granites in Delbar Metamorphic–Igneous Complex, SE of Shahrood (Iran): implications for Neoproterozoic geodynamic evolutions of Central Iran. Journal of Asian Earth Sciences 92, 92–124.

Ballard, J.R., Palin, J.M., Campbell, I.H., 2002. Relative oxidation states of magmas inferred from $Ce^{(IV)}/Ce^{(III)}$ in zircon: application to porphyry copper deposits of northern Chile. Contributions to Mineralogy and Petrology 144, 347–364.

Belousova, E.A., Griffin, W.L., O'Reilly, S.Y., Fisher, N.I., 2002. Igneous zircon: trace element composition as an indicator of source rock type. Contributions to Mineralogy and Petrology 143, 602–622.

Benisek, A., Finger, F., 1993. Factors controlling the development of prism faces in granite zircons: a microprobe study. Contributions to Mineralogy and Petrology 114, 441–451.

Berberian, M., King, G.C.P., 1981. Towards a paleogeography and tectonic evolution of Iran. Canadian Journal of Earth Sciences 18 (2), 210–265.

Boehnke, P., Watson, E.B., Trail, D., Harrison, T.M., Schmitt, A.K., 2013. Zircon saturation re-revisited. Chemical Geology 351, 324–334.

Bosak, P., Jaros, J., Spudil, J., Sulovsky, P., Vaclavek, V., 1998. Salt Plugs in the Eastern Zagros, Iran: Results of Regional Geological Reconnaissance. Geolines, Institute of Geology, Academy of Sciences of the Czech Republic.

Bowring, S.A., Grotzinger, J.P., Condon, D.J., Ramezani, J., Newall, M., Allen, P.A., 2007. Geochronologic constraints of the chronostratigraphic framework of the Neoproterozoic Huqf Supergroup, Sultanate of Oman. American Journal of Science 307, 1097–1145.

Brasier, M., McCarron, G., Tucker, R., Leather, J., Allen, P.A., Shields, G.A., 2000. New U–Pb zircon dates for the Neoproterozoic Ghubrah glaciation and for the top of the Huqf Supergroup, Oman. Geology 28, 175–178.

Caironi, V., Colombo, A., Tunesi, A., Gritti, C., 2000. Chemical variations of zircon compared with morphological evolution during magmatic crystallization: an example from the Valle del Cervo Pluton (Western Alps). European Journal of Mineralogy 12, 779–794.

Carley, T.L., Miller, C.F., Wooden, J.L., Padilla, A.J., Schmitt, A.K., Economos, R.C., Bindeman, I.N., Jordan, B.T., 2014. Iceland is not a magmatic analog for the Hadean: evidence from the zircon record. Earth and Planetary Science Letters 405, 85–97.

Cherniak, D.J., Watson, E.B., 2001. Pb diffusion in zircon. Chemical Geology 172 (1), 5–24.

Das Gupta, S.P., 1996. Marwar Supergroup evaporites, Rajasthan. In: Bhattacharya, A. (Ed.), Recent Advances in Vindhyan Geology. Geological Society of India Memoir 36, pp. 49–58.

De Bockh, H., Lees, G.M., Richardson, F.D.S., 1929. Contribution to the stratigraphy and tectonics of the Iranian Ranges. In: Gregory, J.W. (Ed.), The Structure of Asia, London, Methuen, pp. 58–176.

Elyasi, J., Aminsobhani, E., Behzad, A., Moiinvaziri, H., Meisami, A., 1977. Geology of Hormoz Island. Proceeding of the Second Geological Symposium of Iran. The Iranian Petroleum Institute, Iran, pp. 31–72 (in persian).

Ferry, J.M., Watson, E.B., 2007. New thermodynamic models and revised calibrations for the Ti-in-zircon and Zr-in-rutile thermometers. Contributions to Mineralogy and Petrology 154 (4), 429–437.

Ghavidel-Syooki, M., 1995. Palinostratigraphy and paleogeography of a Paleozoic sequence in the Hasankdar area, central Alborz range, northern Iran. Review of Palaeobotany and Palynology 86, 91–109.

Ghazban, F., Motiei, H., 2007. Petroleum Geology of the Persian Gulf. Tehran University and National Iranian Oil Company, Iran, p. 707.

Griffin, W.L., Wang, X., Jackson, S.E., Pearson, N.J., O'Reilly, S.Y., Xu, X., Zhou, X., 2002. Zircon chemistry and magma mixing, SE China: in situ analysis of Hf isotopes, Tonglu and Pingtan igneous complexes. Lithos 61, 237–269.

Grimes, C.B., John, B.E., Kelemen, P.B., Mazdab, F., Wooden, J.L., Cheadle, M.J., Hanghoj, K., Schwartz, J.J., 2007. Trace element chemistry of zircons from oceanic crust: a method for distinguishing detrital zircon provenance. Geology 35, 643–646.

Harrison, J.V., 1930. The geology of some salt plugs in Laristan (southern Persia). Geological Society of London Quarterly Journal 86, 463–522.

Hassanzadeh, J., Stockli, D.F., Horton, B.K., Axen, G.J., Stockli, L.D., Grove, M., Schmitt, A.K., Walker, J.D., 2008. U–Pb zircon geochronology of late Neoproterozoic–Early Cambrian granitoids in Iran: implications for paleogeography, magmatism, and exhumation history of Iranian basement. Tectonophysics 451, 71–96.

Hastie, A.R., Kerr, A.C., Pearce, J.A., Mitchell, S.F., 2007. Classification of altered volcanic island arc rocks using immobile trace elements: development of the Th–Co discrimination diagram. Journal of Petrology 48, 2341–2357.

Hidaka, H., Shimuzu, H., Adachi, M., 2002. U–Pb geochronology and REE geochemistry of zircons from Paleoproterozoic paragneiss clasts in the Mesozoic Kamiaso conglomerate, central Japan: evidence for an Archean provenance. Chemical Geology l87, 279–293.

Horton, B.K., Hassanzadeh, J., Stockli, D.F., Axen, G.J., Gillis, R.J., Guest, B., Amini, A.H., Fakhari, M., Zamanzadeh, S.M., Grove, M., 2008. Detrital zircon provenance of Neoproterozoic to Cenozoic deposits in Iran: implications for chronostratigraphy and collisional tectonics. Tectonophysics 451, 97–122.

Hoskin, P.W.O., Ireland, T.R., 2000. Rare earth element chemistry of zircon and its use as a provenance indicator. Geology 28, 627–630.

Hoskin, P.W.O., Schaltegger, U., 2004. The composition of zircon and igneous and metamorphic petrogenesis. In: Hanchar, J.M., Hoskin, P.W.O. (Eds.), Zircon: Reviews in

Mineralogy and Geochemistry. Mineralogical Society of America, Washington DC, USA 53, pp. 27–62.
Hoskin, P.W.O., Kinny, P.D., Wyborn, D., Chappell, B.W., 2000. Identifying accessory mineral saturation during differentiation in granitoid magmas: an integrated approach. Journal of Petrology 41, 1365–1396.
Hurford, A.J., Grunau, H.R., Stocklin, J., 1984. Fission track dating of an apatite crystal from Hormoz Island, Iran. Journal of Petroleum Geology 7, 365–380.
Husseini, M.L., 1990. The Cambro-Ordovician Arabian and adjoining plates: a glacio-eustatic model. Journal of Petroleum Geology 133, 267–288.
Kent, P.E., 1970. The salt of the Persian Gulf region. Transactions of the Leicester Literary and Philosophical Society 64, 56–88.
Kumar, V., 1999. Eocambrian sedimentation in Nagaur–Ganganagar evaporite basin, Rajasthan. Journal of the Indian Association of Sedimentologists 18, 201–210.
Lee, J.K.W., Williams, I.S., Ellis, D.J., 1997. Pb, U and Th diffusion in natural zircon. Nature 390, 159–162.
Liaghat, C., 2002. Ground Surface Deformation Induced by Salt Diapirism in oil Field Zones: Some Examples in SE Zagros (Iran). AAPG Annual Meeting, Houston, Texas.
Ludwig, K.R., 2012. Isoplot/Ex Version 4: A Geochronological Toolkit for Microsoft Excel. Berkeley Geochronology Center, special publication 5, 1–75.
McCourt, W.J., Ibrahim, K.M., 1990. The Geology, Geochemistry and Tectonic Setting of the Granitic and Associated Rocks in the Aqapa and Araba Complexes Southwest Jordan, Bulletin Geological Mapping Division 10. Natural Resources Authority, Jordan.
McDonough, W.F., Sun, S.S., 1995. The composition of the Earth. Chemical Geology 120, 223–253.
Nasir, S., Al-Saad, H., Sadooni, F., 2003. Chronostratigraphy and geochemical characterization of volcanic rocks from the Hormuz complex: constraints from the Halul Island, the State of Qatar. Neues Jahrbuch fuer Geologie und Paleontologie Abhandlung 230, 49–66.
Nasir, S., Al-Saad, H., Alsaigh, A., Weidlich, O., 2008. Geology and petrology of the Hormoz dolomite, Infra-Cambrian: implications for the formation of the salt-cored Halul and Shraouh islands, Offshore, State of Qatar. Journal of Asian Earth Sciences 33, 353–365.
Paces, J.B., Miller, J.D., 1993. Precise U–Pb age of Duluth Complex and related mafic intrusions, northeastern Minnesota: geochronological insights into physical, petrogenic, paleomagnetic, and tectonomagnetic processes associated with the 1.1 Ga midcontinent rift systems. Journal of Geophysical Research 98, 13997–14013.
Pearce, J.A., 1982. Trace element characteristics of lavas from destructive plate boundaries. In: Thorpe, R.S. (Ed.), Andesites: Orogenic Andesites and Related Rocks. John Wiley and Sons, Chichester, England, pp. 525–548.
Pearce, J.A., Harris, N.B.W., Tindle, A.G., 1984. Trace element discrimination diagrams for the tectonic interpretation of granitic rocks. Journal of Petrology 25, 956–983.
Pilgrim, G.E., 1908. The geology of the Persian Gulf and the adjoining portion of Persia and Arabia. Memoirs of the Geological Survey of India 34, 1–177.
Pilgrim, G.E., 1924. The geology of parts of the Persian provinces Fars, Kirman and Laristan. Memoirs of the Geological Survey of India 48, 89–111.
Player, R.A., 1969. The Hormuz Salt Plugs of southern Iran PhD Dissertation, Reading University (300 pp.).
Quidelleur, X., Grove, M., Lovera, O.M., Harrison, T.M., Yin, A., Ryerson, F.J., 1997. The thermal evolution and slip history of the Renbu Zedong Thrust, southeastern Tibet. Journal of Geophysical Research 102, 2659–2679.
Ramezani, J., Tucker, R.D., 2003. The Saghand region, central Iran: U–Pb geochronology, petrogenesis and implications for Gondwana tectonics. American Journal of Science 303, 622–665.
Rubatto, D., 2002. Zircon trace element geochemistry: partitioning with garnet and the link between U–Pb ages and metamorphism. Chemical Geology l84, 123–138.
Sánchez-García, T., Bellido, F., Pereira, M.F., Chichorro, M., Quesada, C., Pin, C.H., Silva, J.B., 2010. Rift related volcanism predating the birth of the Rheic Ocean (Ossa-Morena Zone, SW Iberia). Gondwana Research 17, 392–407.
Sano, Y., Terada, K., Fukuoka, T., 2002. High mass resolution ion microprobe analysis of rare earth elements in silicate glass, apatite and zircon: lack of matrix dependency. Chemical Geology 184, 217–230.
Schandl, E.S., Gorton, M.P., 2002. Application of high field strength elements to discriminate tectonic settings in VMS environments. Economic Geology 97, 629–642.
Schmitt, A.K., Grove, M., Harrison, T.M., Lovera, O.M., Hulen, J., Waters, M., 2003. The Geysers–Cobb Mountain Magma System, California (Part 1): U–Pb zircon ages of volcanic rocks, conditions of zircon crystallization and magma residence times. Geochimica et Cosmochimica Acta 67, 3423–3442.
Schröder, S., Schreiber, B.C., Amthor, J.E., Matter, A., 2003. A depositional model for the terminal Neoproterozoic–Early Cambrian Ara Group evaporites in south Oman. Sedimentology 50, 879–898.
Shafaii Moghadam, H., Khademi, M., Hu, Z., Stern, R.J., Santos, J.F., Wu, Y., 2013. Cadomian (Ediacaran–Cambrian) arc magmatism in the ChahJam–Biarjmand metamorphic complex (Iran): magmatism along the northern active margin of Gondwana. Gondwana Research 27, 439–452.
Stacey, J.S., Kramers, J.D., 1975. Approximation of terrestrial lead isotope evolution by a two-stage model. Earth and Planetary Science Letters 26 (2), 207–221.
Stocklin, J., 1968. Salt deposits of the Middle East. Geological Society of America, Special Paper 88, 157–181.
Ustaömer, P.A., Ustaömer, T., Collins, A.S., Robertson, A.H.F., 2009. Cadomian (Ediacaran–Cambrian) arc magmatism in the Bitlis Massif, SE Turkey: magmatism along the developing northern margin of Gondwana. Tectonophysics 473, 99–112.
Wang, X., Griffin, W.L., Chen, J., 2010. Hf contents and Zr/Hf ratios in granitic zircons. Geochemical Journal 44, 65–72.
Wiedenbeck, M., Alle, P., Corfu, F., Griffin, W.L., Meier, M., Oberli, F., Von Quadt, A., Roddick, J.C., Spiegel, W., 1995. Three natural zircon standards for U–Th–Pb, Lu–Hf, trace element and REE analyses. Geostandards Newsletter 19, 1–23.